Int J Clin Exp Pathol 2019;12(2):455-465
www.ijcep.com /ISSN:1936-2625/IJCEP0085116

Original Article

Down-regulation of LncRNA UCA1 alleviates liver injury in rats with liver cirrhosis

Yinhong Zhu[1], Xiaobei Chen[1], Chunhua Zheng[1], Xianlin Rao[1], Xiaomou Peng[2]

[1]*Department of Infectious Diseases, Tongde Hospital of Zhejiang Province, Hangzhou, PR China;* [2]*Department of Infectious Diseases, The Fifth Affiliated Hospital Sun Yat-sen University, Zhuhai, PR China*

Received September 5, 2018; Accepted December 6, 2018; Epub February 1, 2019; Published February 15, 2019

Abstract: Objective: The purpose of this study is to explore the role of long non-coding RNA HULC (lncRNA HULC) in liver injury of rats with cirrhosis. Methods: The rat model of liver cirrhosis was induced by dimethylnitrosamine (DMN), which was intraperitoneally injected with siRNA-negative control (NC) or HULC siRNA. HULC expression in rat liver tissues was detected by qRT-PCR. The amounts of alanine transaminase (ALT) and aspartate aminotransferase (AST) in serum and levels of malonyldialdehyde (MDA) and superoxide dismutase (SOD) in liver tissues were measured. TUNEL staining was used to determine hepatocyte apoptosis. Western blot analysis was used to detect the expression of Caspase-3, Bax, and Bcl-2 in liver tissues. qRT-PCR and ELISA were used to detect the mRNA levels and contents of IL-1β and TNF-α in liver tissues and serum of rats, respectively. Results: High expression of HULC was found in liver tissues of rats with liver cirrhosis. Downregulation of HULC reduced the contents of ALT and AST in serum of rats, inhibited liver tissue lesions and liver fibrosis in rats, suppressed apoptosis (lower expression of caspase-3 and Bax as well as higher BCL-2 expression) of hepatocytes in rats, and inhibited oxidative stress (decreased MDA and increased SOD) and inflammatory injury (decreased IL-1β and TNF-α) in rats with cirrhosis. Conclusion: The findings in this study highlight that the expression of HULC is up-regulated in liver tissues of rats with cirrhosis, and down-regulation of UCA1 could inhibit liver injury in rats with cirrhosis.

Keywords: Liver cirrhosis, UCA1, liver injury, hepatocytes apoptosis, oxidative stress, inflammatory injury

Introduction

Liver cirrhosis is defined as a common end point for different types of chronic liver diseases, such as chronic viral hepatitis resulting from hepatitis B or hepatitis C viral infections, autoimmune hepatitis, biliary disorders, alcoholic or nonalcoholic fatty liver disease, and inherited metabolic defects [1]. The immune-mediated liver damage in these diseases ultimately contributes to cirrhosis regardless of specific etiology [2]. It is acknowledged that the complications of liver cirrhosis include ascites, hepatic encephalopathy, gastroesophageal varices, and renal and cardiac disturbances, which mainly occur as a consequence of hyperdynamic circulation and portal hypertension together with their hemodynamic and metabolic effects [3]. Additionally, hepatic fibrosis is regarded as the primary pathologic basis for chronic liver cirrhosis; and the activated hepatic stellate cells (HSCs) are considered as the main cells involved in liver fibrosis [4, 5]. Based on this, an appropriate diagnosis of cirrhosis is of great importance for the management and treatment of patients with chronic liver diseases [6]. Therefore, it is crucial to seek more effective strategies that could prevent the progression of cirrhosis through identifying the potential mechanisms that underlie cirrhosis.

Recently, it has been suggested that the aberrant expression of some long non-coding RNAs (lncRNAs) functions in a wide range of diseases, especially in cancer biology [7-9]. Besides, lncRNAs have been reported to modulate some vital biological processes, such as proliferation, apoptosis, survival, and differentiation [10-12]. Especially, several lncRNAs seem to be involved in liver fibrosis [13, 14]. For example, the inhibition of growth arrest-specific transcript 5 (GAS5) in liver fibrosis mainly depends on a competing endogenous RNA (ceRNAs) [13]. Highly upregulated in liver cancer (HULC), con-

served in primates, is mainly located on chromosome 6p24.3, which is overexpressed in hepatocellular carcinoma (HCC) [15]. Some studies have demonstrated that HULC was upregulated in a large number of human cancers, and has acted as an oncogene lncRNA in the development and progression of tumors [16, 17]. Meanwhile, a couple of lncRNAs have recently been confirmed to participate in development and progression of HCC, while their associations with liver cirrhosis have not been elucidated [18]. On that basis, this study explores the potential role of lncRNA HULC in liver function injury of rats with liver cirrhosis.

Materials and methods

Ethics statement

All animal procedures were approved by the Institutional Animal Ethics Committee of Tongde Hospital of Zhejiang Province.

Experimental animals and grouping

A total of 48 healthy Sprague-Dawley (SD) rats, weighing 200 ± 20 g, were purchased from Beijing Vital River Laboratory Animal Technology Co., Ltd. (Beijing, China). After adaptive feeding for 1 week, the rats were kept in a clean-grade animal room with the temperature of 22-24°C, 12 h day/night cycle, as well as free access to food and drink. The rats were randomly divided into 4 groups according to their body weights, with 12 rats in each group: normal group (intraperitoneal injection of normal saline once a day, 3 days per week, totalling 4 weeks, and injection of phosphate buffer saline (PBS) every other day from the 5th week for 2 weeks), dimethylnitrosamine (DMN) group (a daily intraperitoneal injection of 0.5% v/v)/2 ml/kg of DMN for 3 consecutive days per week, for totally 4 weeks [19], DMN + siRNA-negative control (NC) group (a daily intraperitoneal injection of 0.5% v/v)/2 ml/kg of DMN for 3 consecutive days per week, for totally 4 weeks, and injection of siRNA-NC every other day from the 5th week for 2 weeks) and DMN + HULC-siRNA (a daily intraperitoneal injection of 0.5% v/v)/2 ml/kg of DMN for 3 consecutive days per week, for totally 4 weeks, and injection of HULC-siRNA every other day from the 5th week for 2 weeks). DMN was purchased from Tokyo Kasei Kogyo Co., Ltd. (Tokyo, Japan), and siRNA-NC and HULC-siRNA plasmids was purchased from Shanghai Sangon Bioengineering Co., Ltd. (Shanghai, China).

Specimen collection and index detection

Subsequently, rats in each group were anesthetized by intraperitoneal injection of pentobarbital sodium to extract the jugular vein blood. After resting for 30 min, the blood was centrifuged for 10 min at 1500 r/min. The supernatant was stored in the refrigerator at -70°C for the detection of serum indexes. The liver tissues of 4 rats were taken for transmission electron microscope observation, and the liver tissues of 4 rats were fixed in 4% paraformaldehyde solution, routinely dehydrated, paraffin embedded and sectioned for histological examination. The liver tissues of the remaining 4 rats were stored in -80°C cryogenic refrigerator for the detection of quantitative reverse transcription polymerase chain reaction (qRT-PCR), western blot analysis and oxidative stress index.

The contents of alanine transaminase (ALT) and aspartate aminotransferase (AST) in serum were calculated by spectrophotometry according to the instructions of the kit (Nanjing Jiancheng Bioengineering Institute, Nanjing, Jiangsu, China).

The expression levels of IL-6, IL-8, and TNF-α in serum (Nanjing Jiancheng Bioengineering Institute, Nanjing, Jiangsu, China) were detected by enzyme-linked immunosorbent assay (ELISA).

The levels of oxidative stress index, malonyldialdehyde (MDA) and superoxide dismutase (SOD) (Nanjing Jiancheng Bioengineering Institute, Nanjing, Jiangsu, China) in homogenate of liver tissues were measured by spectrophotometer colorimetry.

Transmission electron microscope observation

Small pieces of fresh liver tissues used for transmission electron microscope observation were taken and immobilized in 4% glutaraldehyde precooled at 4°C for 24 h. The tissues were then immobilized with 1% osmitic acid for 2 h, dehydrated with conventional ethanol and acetone, encapsulated with acetone-Epon812 epoxy resin, sliced into ultrathin section, stained with uranium acetate and lead citrate

Table 1. Primer sequence

Gene	Sequence
HULC	F: 5'-GGGGGTGGAACTCATGATGG-3'
	R: 5'-TGGGAAGCATGGCAAAATATCA-3'
IL-1β	F: 5'-GAAGGCAGTGTCACTCATT-3'
	R: 5'-TCTTTGGGTATTGTTTGG-3'
TNF-α	F: 5'-CTGTGAAGGGAATGGGTGTT-3'
	R: 5'-GGGCTGGCTCTGTGAGGAAG-3'
GAPDH	F: 5'-CGACT-TCAACAGCAACTCCCACTCTTCC-3'
	R: 5'-TGGGTGGTCCAGGGTTTCTTACTCCTT-3'

Note: F, forward; R, reverse; GAPDH, glyceraldehyde phosphate dehydrogenase.

electron, and the ultrastructure was observed by a transmission electron microscope.

Hematoxylin-eosin (HE) staining

More than 3 sections of liver tissues from each rat of each group were dewaxed and hydrated. After H&E staining, the histopathological examination was performed and photos were taken so as to observe the histopathological condition in liver tissues of rats in each group.

Masson staining

No less than 3 sections of each rat were taken from each group. The slices were routinely dewaxed, hydrated, stained with Masson compound dyeing solution for 5 min, washed with distilled water, stained with molybdic acid for 5 min, then dried, stained with aniline blue for 5 min, and slightly flushed with distilled water, differentiated with differentiation liquid for 30~60 s (twice), dehydrated, cleared, sealed by neutral gum. Collagen fibers were blue, nuclei were blue, as well as cytoplasm, muscle fibers and red blood cells were red. Three visual fields were taken from each slice and the fibers were semi-quantified by Image J software National Institutes of Health, Bethesda, Maryland, USA.

Terminal deoxynucleotidyl transferase (TdT)-mediated dUTP nick end labeling (TUNEL) staining

No less than 3 sections of each rat were taken from each group. Apoptosis of hepatocytes was detected by TUNEL kit (Wuhan Boster Biological Technology LT, Wuhan, China). The sections were observed under a microscope. The cells with brown granules in the nucleus were apoptotic cells. According to the staining results, five high-power visual fields (× 400 times) with the largest number of positive cells were randomly selected from each section, and the percentage of positive cells in 500 hepatocytes was calculated as apoptotic index (AI).

qRT-PCR

The one-step method of Trizol (Invitrogen, Carlsbad, CA, USA) was adopted for the extraction of the total RNA of tissues and cells, and the high-quality RNA was verified by ultraviolet (UV) analysis together with formaldehyde denaturation electrophoresis detection. With the obtain of 1 μg RNA, cDNA was obtained by the reverse transcription of avian myeloblastosis virus (AMV). As shown in **Table 1**, PCR primer was designed and synthesized by Invitrogen, Carlsbad, CA, USA. U6 and glyceraldehyde phosphate dehydrogenase (GAPDH) were used as internal controls. The amplification conditions for PCR were shown as follows: pre-denaturation at 94°C for 5 min, with a total of 40 cycles of denaturation at 94°C for 40 s, annealing at 60°C for 40 s, extension at 72°C for 1 min and finally, extension at 72°C for 10 min. The PCR product was verified by agarose gel electrophoresis. Through manually selecting the threshold at the lowest point of parallel rise of each logarithmic expansion curve, the threshold cycle (Ct) value of each reaction tube was obtained. $2^{-\Delta\Delta Ct}$ method was utilized for analyzing the ratio relation of target gene expression between the experimental group and the control group. The formula is as follows: $\Delta\Delta Ct = [Ct_{(\text{target gene})} - Ct_{(\text{internal control gene})}]_{\text{the experimental group}} - [Ct_{(\text{target gene})} - Ct_{(\text{internal control gene})}]_{\text{the control group}}$. The experiment was done independently 3 times to obtain the average value.

Western blot analysis

The proteins from cells were extracted and the protein concentrations were determined based on the instructions of the bicinchoninic acid (BCA) assay (Wuhan Boster Biological Technology LT, Wuhan, China). The extracted protein was supplemented to the sample buffer and subsequently, boiled at 95°C for 10 min, with each well loading 30 μg protein. The proteins were separated by 10% sodium dodecyl sulfate polyacrylamide gel electrophoresis (SDS-PAGE) (Wuhan Boster Biological Technology LT, Wuhan, China), and then trans-

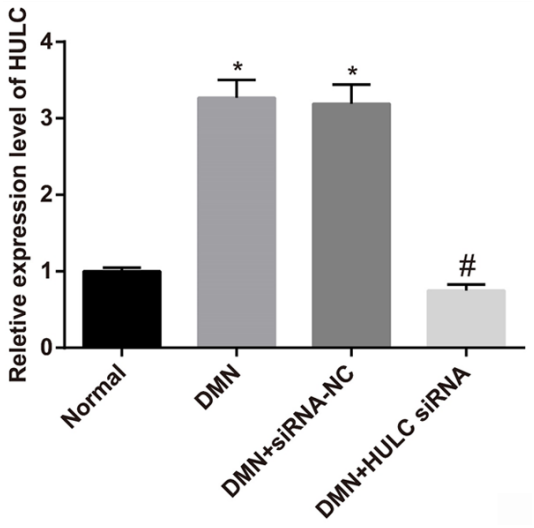

Figure 1. Expression level of HULC in liver tissues of rats in each group. Note: N = 4; the ANOVA was used for the comparison among three or more groups. After ANOVA analysis, the LSD-t test was employed for pairwise comparisons; *P < 0.05 vs. the normal group; #P < 0.05 vs. the DMN group.

ferred to a nitrocellulose membrane by wet transfer method, with the electrophoretic voltage from 80 v to 120 v, the transmembrane voltage of 100 mv as well as the time for 45-70 min. Subsequently, the protein samples were transferred to polyvinylidene fluoride (PVDF) membrane and blocked with 5% bovine serum albumin (BSA) for 1 h. Afterwards, the membranes were supplemented with the primary antibodies to caspase-3, Bax, Bcl-2 (1:1000; Abcam, Cambridge, MA, USA) and β-actin (1:3000; Abcam, Cambridge, MA, USA) and incubated at 4°C overnight. The membranes were rinsed with Tris-buffered saline and Tween 20 (TBST) for 3 times, each time for 5 min, and the corresponding secondary antibodies, which were purchased from Shanghai Miao Tong Biotechnology Company (Shanghai, China), were incubated at room temperature for 1 h in order to wash the membranes for 3 times, each time for 5 min. β-actin was used as an internal control. An electrogenerated chemiluminescence (ECL) reagent and Bio-rad Gel Dol EZ formatter (GEL DOC EZ IMAGER, Bio-Rad, California, USA) were used for developing. The gray value analysis of the target band was analyzed by Image J software (National Institutes of Health, Bethesda, Maryland, USA). The experiment was repeated for three times to obtain the average value.

Statistical analysis

All the data in this study were analyzed by SPSS 21.0 (IBM SPSS Inc. Chicago, IL, USA) software. The data had a normal distribution after being verified by the Kolmogorov-Smirnov test. The results were expressed as mean ± standard deviation. The t test was used for the comparison between two groups, while the one-way analysis of variance (ANOVA) was used for the comparison among three or more groups. After ANOVA analysis, the Fisher's least significant difference t test (LSD-t) was employed for pairwise comparisons. All tests were 2-sided, and P values ≤ 0.05 were considered significant.

Results

High expression of HULC is found in liver tissues of rats with cirrhosis

First, the expression of HULC in rat liver tissues was detected by qRT-PCR. The results showed that the expression level of HULC in the DMN group was significantly increased compared with the normal group (P < 0.05), which suggested that the expression of HULC was involved in cirrhosis induced by DMN. No significant difference was found in the expression level of HULC between the DMN group and the DMN + siRNA-NC group (P > 0.05). In comparison to the DMN + siRNA-NC group, the expression level of HULC in rat liver tissues was significantly decreased (P < 0.05), indicating that HULC-siRNA could effectively inhibit the expression of HULC in liver tissues of rats with cirrhosis (**Figure 1**).

Downregulation of HULC reduces the contents of ALT and AST in serum of rats with cirrhosis

Next, the contents of ALT and AST in serum of rats with cirrhosis were measured by qRT-PCR. As shown in **Figure 2**, the findings indicated that relative to the normal group, the contents of ALT and AST in serum of rats in the DMN group were significantly increased (both P < 0.05). There was no significant difference in the content of ALT and AST in the serum of rats between the DMN group and the DMN + siRNA-NC group (both P > 0.05). The contents of ALT and AST in serum of rats were significantly increased in contrast to the DMN and the DMN + siRNA-NC groups, (all P < 0.05). These results suggest that inhibiting the expression of HULC

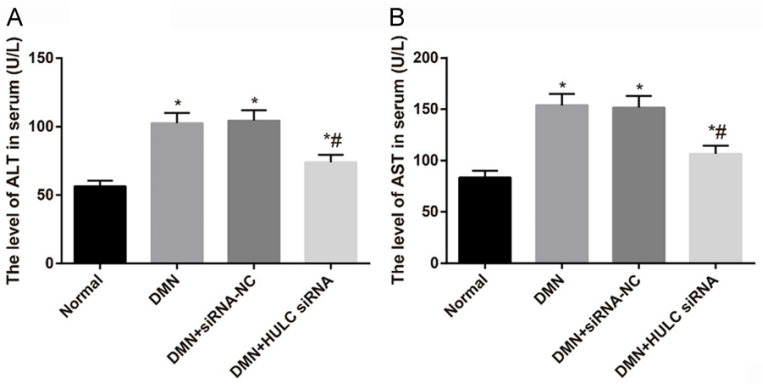

Figure 2. The contents of ALT and AST in serum of rats in each group. Note: A. Determination of ALT in serum of rats in each group by spectrophotometry; B. Determination of AST in serum of rats in each group by spectrophotometry; N = 12, the ANOVA was used for the comparison among three or more groups. After ANOVA analysis, the LSD-t test was employed for pairwise comparisons; *P < 0.05 vs. the normal group; #P < 0.05 vs. the DMN group.

can significantly decrease the levels of ALT and AST in rats with cirrhosis.

Downregulation of HULC inhibits liver tissue lesions and fibrosis in rats with cirrhosis

The findings by H&E staining (**Figure 3A**) showed that the rats in the normal group had clear hepatic lobule structure as well as normal structure of the central vein and confluence area; the hepatic cell cords were arranged radially from the central vein to all sides and there were irregular hepatic sinuses. In rats of the DMN group, there were typical changes of liver cirrhosis, extensive fibrous hyperplasia of liver interstitial tissue, many pseudolobules, and diffuse inflammatory cell infiltrates in interstitial tissue. Similar to the DMN group, the rats in the DMN + siRNA-NC had severe hyperplasia and obvious liver cell degeneration and inflammatory necrosis. In the DMN + HULC siRNA group, the fibrous tissue spacing was normal in rats, and the denaturation and inflammatory reaction necrosis were less than those in the DMN group and the DMN siRNA-NC group.

The results of Masson staining (**Figure 3B**) showed that the normal group of rats presented with normal liver tissue structure and no fibrous deposition; the proliferation of hepatic fibrous tissue was obvious, and a coarse fiber spacing was formed in rats of the DMN group and the DMN siRNA-NC group; the liver fibrosis in rats was significantly reduced in the DMN siRNA-NC group. In comparison to the DMN group and the DMN siRNA-NC group, the area of liver collagen decreased significantly in the DMN siRNA-NC group (both P < 0.05).

The results of transmission electron microscope observation (**Figure 3C**) showed that the hepatocytes in rats of the normal group were clear in structure, abundant in cytoplasm, intact in nuclear membrane, dense in nucleoli, and distributed in groups of rough endoplasmic reticulum in the cytoplasm and arranged in stratified order. The hepatocytes in rats of the DMN group and the DMN siRNA-NC group presented with deformed nucleus, loose nucleolus, condensation of heterochromatin in nucleus, cavitation of nuclear matrix, large lipid droplets in cytoplasm, obvious dilatation of capillary bile ducts, unclear wall structure, more vacuoles in cytoplasm, swelling of mitochondria,and cystic dilatation and fracture of rough surfaced endoplasmic reticulum (RER). The hepatocytes in rats of the DMN + HULC siRNA group showed mild swelling, partial mitochondrial proliferation, and endoplasmic reticulum slightly dilated. This suggests that inhibiting the expression of HULC can improve the pathological changes of liver tissues in rats with liver cirrhosis.

Inhibition of HULC suppresses apoptosis of hepatocytes in rats with liver cirrhosis

The results of TUNEL staining showed that there were few apoptotic hepatocytes in the liver tissues of rats in the normal group. Compared with the normal group, the AI of hepatocytes was increased significantly in the DMN group and the DMN siRNA-NC group (both P < 0.05). The AI of hepatocytes in the DMN + HULC siRNA group was significantly lower than that in the DMN group and the DMN siRNA-NC group (both P < 0.05; **Figure 4A**).

Western blot analysis demonstrated that the expression of caspase-3 and Bax was significantly upregulated while the expression of Bcl-2 was remarkably downregulated in liver tissues of rats in the DMN group and the DMN

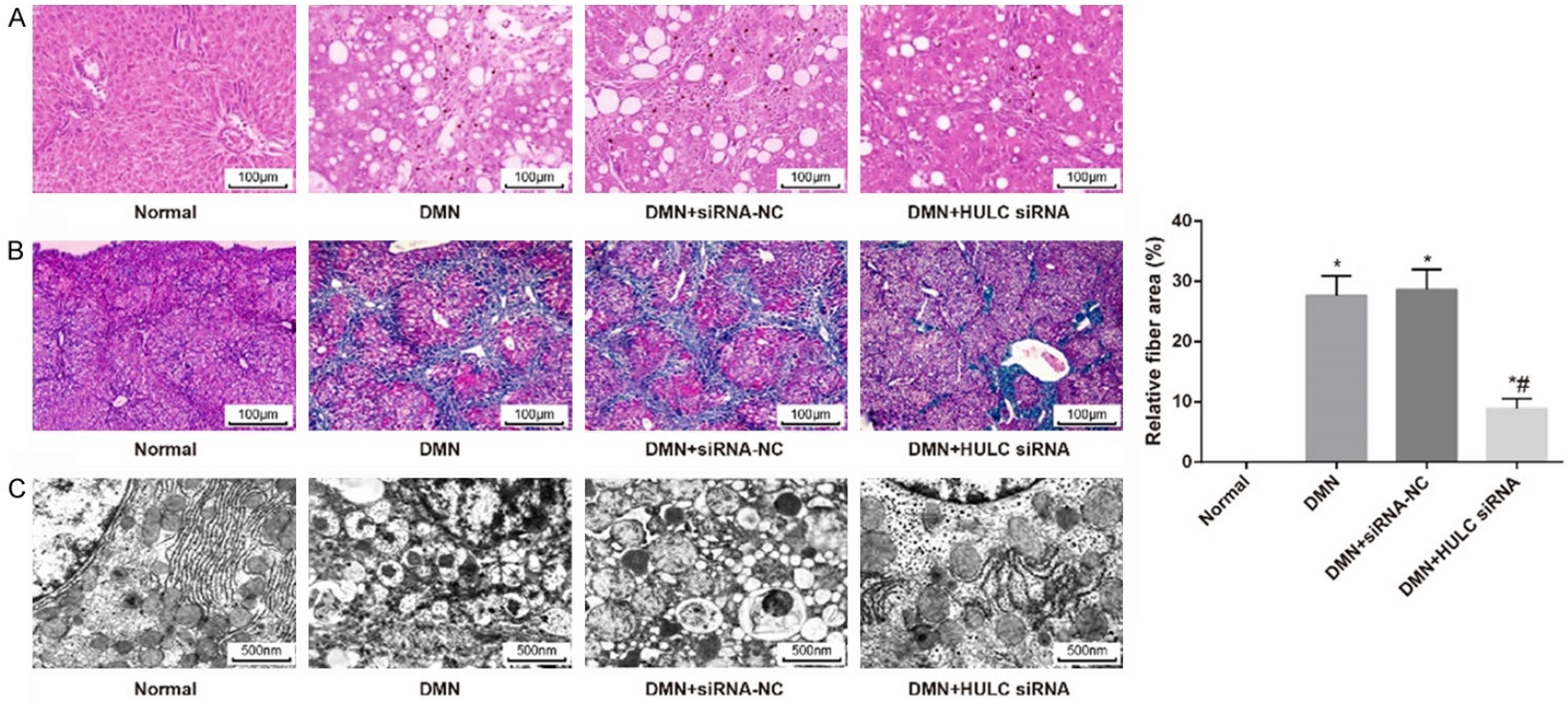

Figure 3. Changes of histopathology in liver and ultrastructure in hippocampus of rats in each group. Note: N = 4; A. Liver tissue morphology in each group by H&E staining (× 100); B. Determination of hepatic fibrosis in rats by Masson staining (× 100); C. Ultrastructure of hippocampal tissue of rats in each group (× 20000); *P < 0.05 vs. the normal group; #P < 0.05 vs. the DMN group.

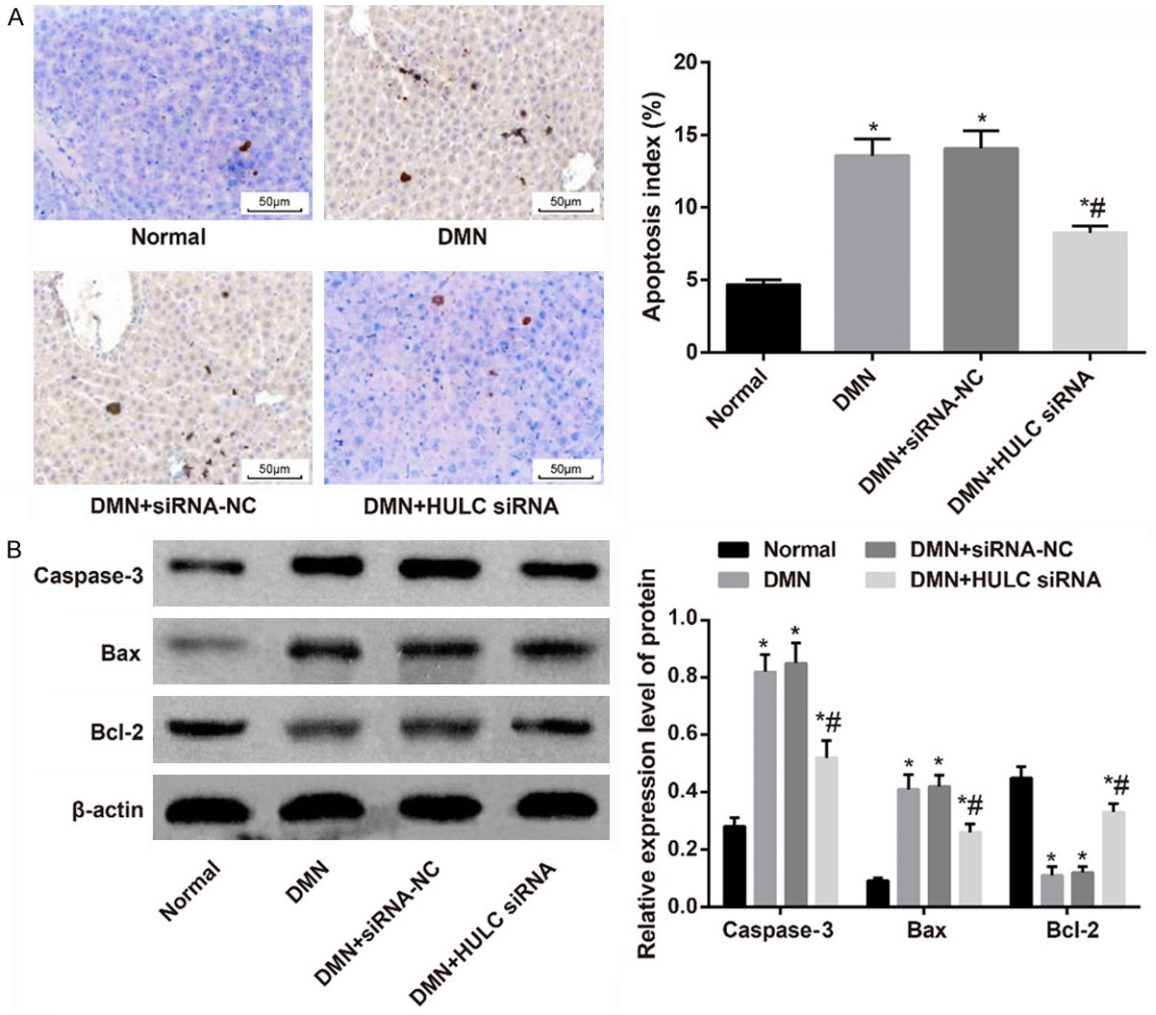

Figure 4. Apoptosis of rat hepatocytes in each group. Note: N = 4; A. TUNEL staining for the detection of hepatocyte apoptosis in rats in each group (× 200); B. The expression level of apoptosis-related protein in liver tissues of each group was detected by western blot analysis; the ANOVA was used for the comparison among three or more groups. After ANOVA analysis, the LSD-t test was employed for pairwise comparisons; *$P < 0.05$ vs. the normal group; #$P < 0.05$ vs. the DMN group.

siRNA-NC group compared to the normal group (all $P < 0.05$). The expression of caspase-3 and Bax in liver tissues of rats in the DMN + HULC siRNA group was significantly lower while the expression of Bcl-2 was remarkably higher than those in the DMN group and the DMN + siRNA-NC group (all $P < 0.05$; **Figure 4B**).

Inhibition of HULC inhibits oxidative stress and inflammatory injury in rats with cirrhosis

Subsequently, the levels of MDA and SOD in liver tissues of each group were measured. The results showed that the level of MDA in liver tissues was increased significantly and the level of SOD was decreased significantly in the DMN group and the DMN + siRNA-NC group in contrast to the normal group (all $P < 0.05$). Relative to the DMN group and the DMN + siRNA-NC group, the level of MDA in liver tissues of rats was decreased significantly and the level of SOD was increased significantly in the DMN + HULC siRNA group (all $P < 0.05$; **Figure 5A**, **5B**), suggesting that inhibiting the expression of HULC could inhibit oxidative stress injury in rats with liver cirrhosis.

The mRNA expression of inflammatory factors IL-1β and TNF-α in liver tissues of each group was detected by qRT-PCR. The results suggested that the mRNA expression of IL-1β and TNF-α in liver tissues of rats in the DMN group was increased significantly compared with the normal group (both $P < 0.05$). The mRNA expres-

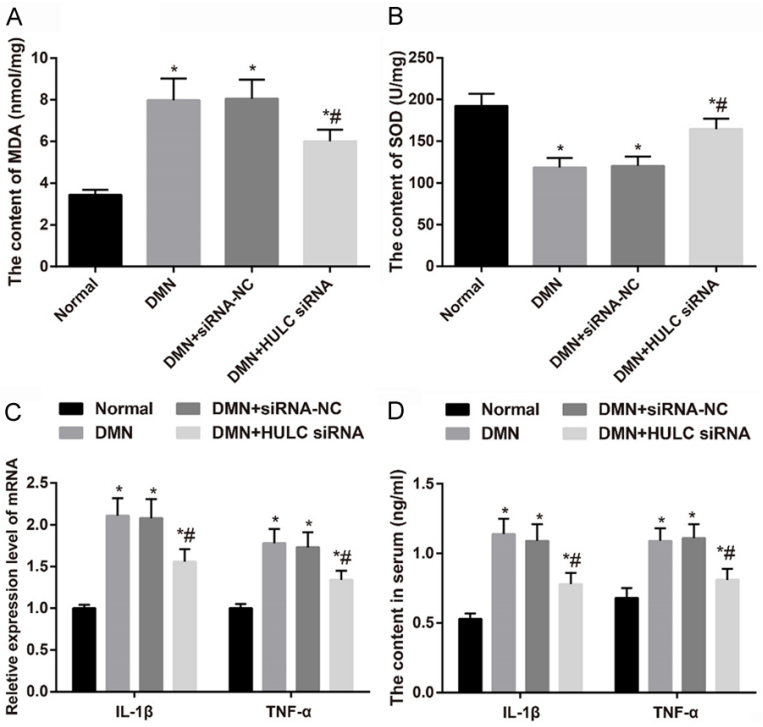

Figure 5. Oxidative stress and inflammatory injury in each group of rats. Note: A. Determination of MDA level in liver tissues of rats in each group by spectrophotometric colorimetry, N = 4; B. Determination of SOD levels in liver tissues of rats by spectrophotometric colorimetry, N = 4; C. mRNA expression of inflammatory factors in liver tissues of rats in each group detected by qRT-PCR, N = 4; D. Detection of the expression of inflammatory factors in serum of rats in each group by ELISA, N = 12; the ANOVA was used for the comparison among three or more groups. After ANOVA analysis, the LSD-t test was employed for pairwise comparisons; **P* < 0.05 vs. the normal group; #*P* < 0.05 vs. the DMN group.

sion of IL-1β and TNF-α in liver tissues of rats in the DMN group and the DMN + siRNA-NC group was not significantly different (all $P > 0.05$), but the mRNA expression of IL-1β and TNF-α in liver tissues of rats in the DMN + HULC siRNA group was significantly lower than that in the DMN + siRNA-NC group (both $P < 0.05$; **Figure 5C**).

Furthermore, the contents of IL-1β and TNF-α in serum of rats in each group were detected by ELISA. The results revealed that there was no significant difference in the content of IL-1β and TNF-α in serum of rats in the DMN and DMN + siRNA-NC groups (all $P > 0.05$). The content of IL-1β and TNF-α in serum of rats in the DMN group and the DMN + siRNA-NC group was significantly higher than those in the normal group (all $P < 0.05$), but the content of IL-1β and TNF-α in serum of rats in the DMN + HULC siRNA group was markedly lower than that in the DMN + siRNA-NC group (both $P < 0.05$; **Figure 5D**).

Discussion

LncRNAs, as a novel type of RNA with limited or no protein coding ability, have been reported to be implicated in a growing number of cellular processes and essential functions in cancer biology [20-22]. HULC, a lncRNA overexpressed in HCC, has been shown to be participated in the carcinogenesis and progression of HCC [23]. However, the mechanisms of HULC in functional impairment in liver cirrhosis are still not well elucidated. Therefore, in this present study, we aim to figure out whether HULC plays a significant part in liver function injury of liver cirrhosis.

One of the findings in our study suggested that high expression of HULC was found in liver tissues of rats with liver cirrhosis. HULC is a lncRNA initially identified in HCC, that is significantly overexpressed in human HCC samples [15]. Recently, it is reported that HULC is related to several other types of cancers, including nasopharyngeal carcinoma, gastric cancer, andcolorectal carcinoma [24-26]. Panzitt et al. have found that using cDNA arrays and RT-PCR, HULC was the most upregulated in HCC [15]. Also, a previous study revealed that HULC was overexpressed in HCC and had a close association with the staging and grading of HCC [27]. Yang et al. showed that HULC overexpression was a favorable factor for overall survival (OS) and disease-free survival (DFS) in HCC patients [28]. Moreover, high expression of HULC has been suggested to be a prognostic biomarker for poor OS and metastasis in some general human tumors [29]. Collectively, all these aforementioned reasons led us to the confirmation of the hypothesis that overexpression of HULC participated in the progression of liver cirrhosis.

Our study also suggested that downregulation of HULC reduced the contents of ALT and AST in

serum of rats, inhibited liver tissue lesions and liver fibrosis in rats, and suppressed apoptosis of hepatocytes (lower expression of caspase-3 and Bax as well as higher Bcl-2 expression) in rats with liver cirrhosis. Serum ALT and AST levels are used as sensitive markers of tissue damage, especially liver toxicity [30, 31]. Similar to our results, a previous study has demonstrated the hepatic function indexes, ALT and AST, were reduced by si-NEAT1 lentivirus in high-fat diet (HFD) rats with non-alcoholic fatty liver disease [32]. Besides, it has been reported that the effect of expression of MALAT-1 on cell growth, cell cycle entry, and invasion mainly depends on the regulation of expression of apoptotic genes (i.e., caspase-3, Bax, and Bcl-2) [33, 34]. Furthermore, the inhibition of HULC is demonstrated to restrict cell proliferation and induce apoptosis in several tumors, and HULC could act as a useful biomarker for the diagnosis and prognosis of tumors [35]. The results of our study demonstrated that downregulation of HULC inhibited oxidative stress (decreased MDA and increased SOD) and inflammatory injury (decreased IL-1β and TNF-α) in rats with liver cirrhosis. A previous study has demonstrated that hypoxic PC12 cells had an elevation in MDA with increased apoptotic cells, while a reduction in SOD in cells treated with MALAT-1, indicating downregulation of MALAT-1 can inhibit the oxidative stress of PC12 cells through activating the p38MAPK pathway [36]. Howeverf, Chen et al. have proposed that MALAT1 knockdown significantly decreased levels of TNF-α, IL-1β, IL-6, IL-10, IL-17, as well as IFN-γ [37], which is in accordance with the results in our study.

In summary, the present study has provided evidence highlighting the role of HULC in liver cirrhosis. It is suggested that the expression of HULC is up-regulated in liver tissues of rats with liver cirrhosis; and the down-regulation of UCA1 could inhibit liver injury in rats with liver cirrhosis, suggesting HULC could be used as an important indicator for the treatment of liver cirrhosis. However, this study focused only on animals; in vitro experiments would be helpful for confirmation of our findings, which could be performed in future.

Acknowledgements

We would like to acknowledge the reviewers for their helpful comments on this paper. Study on the relationship between the formation mechanism of hepatic lesion sensitive phase and the growth and decline pattern of HBV core associated antigen was supported by the National Natural Science Foundation of China (Grant No. 81071366).

Disclosure of conflict of interest

None.

Address correspondence to: Dr. Yinhong Zhu, Department of Infectious Diseases, Tongde Hospital of Zhejiang Province, 234 Gucui Road, Xihu District, Hangzhou 321012, Zhejiang Province, PR China. Tel: +86-571-89972442; E-mail: zhuyinhong620@163.com

References

[1] Tsochatzis EA, Bosch J, Burroughs AK. Liver cirrhosis. Lancet 2014; 383: 1749-1761.

[2] Harring TR, Guiteau JJ, Nguyen NT, Cotton RT, Gingras MC, Wheeler DA, O'Mahony CA, Gibbs RA, Brunicardi FC, Goss JA. Building a comprehensive genomic program for hepatocellular carcinoma. World J Surg 2011; 35: 1746-1750.

[3] Sekiya Y, Ogawa T, Yoshizato K, Ikeda K, Kawada N. Suppression of hepatic stellate cell activation by microRNA-29b. Biochem Biophys Res Commun 2011; 412: 74-79.

[4] Higashi T, Friedman SL, Hoshida Y. Hepatic stellate cells as key target in liver fibrosis. Adv Drug Deliv Rev 2017; 121: 27-42.

[5] Li XQ, Ren ZX, Li K, Huang JJ, Huang ZT, Zhou TR, Cao HY, Zhang FX, Tan B. Key anti-fibrosis associated long noncoding RNAs identified in human hepatic stellate cell via transcriptome sequencing analysis. Int J Mol Sci 2018; 19.

[6] Ganne-Carrié N, Ziol M, de Ledinghen V, Douvin C, Marcellin P, Castera L, Dhumeaux D, Trinchet JC, Beaugrand M. Accuracy of liver stiffness measurement for the diagnosis of cirrhosis in patients with chronic liver diseases. Hepatology 2006; 44: 1511-1517.

[7] Gutschner T and Diederichs S. The hallmarks of cancer: a long non-coding RNA point of view. RNA Biol 2012; 9: 703-719.

[8] Lv QL, Hu L, Chen SH, Sun B, Fu ML, Qin CZ, Qu Q, Wang GH, He CJ, Zhou HH. A long noncoding RNA ZEB1-AS1 promotes tumorigenesis and predicts poor prognosis in glioma. Int J Mol Sci 2016; 17.

[9] Wang J, Liu X, Wu H, Ni P, Gu Z, Qiao Y, Chen N, Sun F, Fan Q. CREB up-regulates long non-coding RNA, HULC expression through interaction with microRNA-372 in liver cancer. Nucleic Acids Res 2010; 38: 5366-5383.

[10] Fatica A and Bozzoni I. Long non-coding RNAs: new players in cell differentiation and development. Nat Rev Genet 2014; 15: 7-21.
[11] Cao C, Sun J, Zhang D, Guo X, Xie L, Li X, Wu D, Liu L. The long intergenic noncoding RNA UFC1, a target of MicroRNA 34a, interacts with the mRNA stabilizing protein HuR to increase levels of beta-catenin in HCC cells. Gastroenterology 2015; 148: 415-426, e418.
[12] Wang F, Yuan JH, Wang SB, Yang F, Yuan SX, Ye C, Yang N, Zhou WP, Li WL, Li W, Sun SH. Oncofetal long noncoding RNA PVT1 promotes proliferation and stem cell-like property of hepatocellular carcinoma cells by stabilizing NOP2. Hepatology 2014; 60: 1278-1290.
[13] Yu F, Zheng J, Mao Y, Dong P, Lu Z, Li G, Guo C, Liu Z, Fan X. Long non-coding RNA growth arrest-specific transcript 5 (GAS5) inhibits liver fibrogenesis through a mechanism of competing endogenous RNA. J Biol Chem 2015; 290: 28286-28298.
[14] Zheng J, Dong P, Mao Y, Chen S, Wu X, Li G, Lu Z, Yu F. lincRNA-p21 inhibits hepatic stellate cell activation and liver fibrogenesis via p21. FEBS J 2015; 282: 4810-4821.
[15] Panzitt K, Tschernatsch MM, Guelly C, Moustafa T, Stradner M, Strohmaier HM, Buck CR, Denk H, Schroeder R, Trauner M, Zatloukal K. Characterization of HULC, a novel gene with striking up-regulation in hepatocellular carcinoma, as noncoding RNA. Gastroenterology 2007; 132: 330-342.
[16] Kitagawa M, Kitagawa K, Kotake Y, Niida H, Ohhata T. Cell cycle regulation by long noncoding RNAs. Cell Mol Life Sci 2013; 70: 4785-4794.
[17] Parasramka MA, Maji S, Matsuda A, Yan IK, Patel T. Long non-coding RNAs as novel targets for therapy in hepatocellular carcinoma. Pharmacol Ther 2016; 161: 67-78.
[18] Zhao J, Fan Y, Wang K, Ni X, Gu J, Lu H, Lu Y, Lu L, Dai X, Wang X. LncRNA HULC affects the differentiation of treg in HBV-related liver cirrhosis. Int Immunopharmacol 2015; 28: 901-905.
[19] Xiang Y, Pang BY, Zhang Y, Xie QL, Zhu Y, Leng AJ, Lu LQ, Chen HL. Effect of Yi Guan Jian decoction on differentiation of bone marrow mesenchymalstem cells into hepatocyte-like cells in dimethylnitrosamine-induced liver cirrhosis in mice. Mol Med Rep 2017; 15: 613-626.
[20] Matsui M and Corey DR. Non-coding RNAs as drug targets. Nat Rev Drug Discov 2017; 16: 167-179.
[21] Hu G, Niu F, Humburg BA, Liao K, Bendi S, Callen S, Fox HS, Buch S. Molecular mechanisms of long noncoding RNAs and their role in disease pathogenesis. Oncotarget 2018; 9: 18648-18663.
[22] Fu M, Zou C, Pan L, Liang W, Qian H, Xu W, Jiang P, Zhang X. Long noncoding RNAs in digestive system cancers: functional roles, molecular mechanisms, and clinical implications (review). Oncol Rep 2016; 36: 1207-1218.
[23] Xiong H, Li B, He J, Zeng Y, Zhang Y, He F. lncRNA HULC promotes the growth of hepatocellular carcinoma cells via stabilizing COX-2 protein. Biochem Biophys Res Commun 2017; 490: 693-699.
[24] Jiang X and Liu W. Long noncoding RNA highly upregulated in liver cancer activates p53-p21 pathway and promotes nasopharyngeal carcinoma cell growth. DNA Cell Biol 2017; 36: 596-602.
[25] Jin C, Shi W, Wang F, Shen X, Qi J, Cong H, Yuan J, Shi L, Zhu B, Luo X, Zhang Y, Ju S. Long noncoding RNA HULC as a novel serum biomarker for diagnosis and prognosis prediction of gastric cancer. Oncotarget 2016; 7: 51763-51772.
[26] Yang XJ, Huang CQ, Peng CW, Hou JX, Liu JY. Long noncoding RNA HULC promotes colorectal carcinoma progression through epigenetically repressing NKD2 expression. Gene 2016; 592: 172-178.
[27] Hämmerle M, Gutschner T, Uckelmann H, Ozgur S, Fiskin E, Gross M, Skawran B, Geffers R, Longerich T, Breuhahn K, Schirmacher P, Stoecklin G, Diederichs S. Posttranscriptional destabilization of the liver-specific long noncoding RNA HULC by the IGF2 mRNA-binding protein 1 (IGF2BP1). Hepatology 2013; 58: 1703-1712.
[28] Yang Z, Lu Y, Xu Q, Tang B, Park CK, Chen X. HULC and H19 played different roles in overall and disease-free survival from hepatocellular carcinoma after curative hepatectomy: a preliminary analysis from gene expression omnibus. Dis Markers 2015; 2015: 191029.
[29] Chen X, Lun L, Hou H, Tian R, Zhang H, Zhang Y. The value of lncRNA HULC as a prognostic factor for survival of cancer outcome: a meta-analysis. Cell Physiol Biochem 2017; 41: 1424-1434.
[30] Kobayashi A, Suzuki Y, Kuno H, Sugai S, Sakakibara H, Shimoi K. Effects of fenofibrate on plasma and hepatic transaminase activities and hepatic transaminase gene expression in rats. J Toxicol Sci 2009; 34: 377-387.
[31] Gao M, Cheng Y, Zheng Y, Zhang W, Wang L, Qin L. Association of serum transaminases with short- and long-term outcomes in patients with ST-elevation myocardial infarction undergoing primary percutaneous coronary intervention. BMC Cardiovasc Disord 2017; 17: 43.
[32] Wang X. Down-regulation of lncRNA-NEAT1 alleviated the non-alcoholic fatty liver disease via mTOR/S6K1 signaling pathway. J Cell Biochem 2018; 119: 1567-1574.

[33] Guo F, Li Y, Liu Y, Wang J, Li Y, Li G. Inhibition of metastasis-associated lung adenocarcinoma transcript 1 in CaSki human cervical cancer cells suppresses cell proliferation and invasion. Acta Biochim Biophys Sin (Shanghai) 2010; 42: 224-229.

[34] Schmidt LH, Görlich D, Spieker T, Rohde C, Schuler M, Mohr M, Humberg J, Sauer T, Thoenissen NH, Huge A, Voss R, Marra A, Faldum A, Müller-Tidow C, Berdel WE, Wiewrodt R. Prognostic impact of Bcl-2 depends on tumor histology and expression of MALAT-1 lncRNA in non-small-cell lung cancer. J Thorac Oncol 2014; 9: 1294-1304.

[35] Ma Z, Huang H, Xu Y, He X, Wang J, Hui B, Ji H, Zhou J, Wang K. Current advances of long noncoding RNA highly upregulated in liver cancer in human tumors. Onco Targets Ther 2017; 10: 4711-4717.

[36] Yang L, Xu F, Zhang M, Shang XY, Xie X, Fu T, Li JP, Li HL. Role of LncRNA MALAT-1 in hypoxia-induced PC12 cell injury via regulating p38MAPK signaling pathway. Neurosci Lett 2018; 670: 41-47.

[37] Chen H, Wang X, Yan X, Cheng X, He X, Zheng W. LncRNA MALAT1 regulates sepsis-induced cardiac inflammation and dysfunction via interaction with miR-125b and p38 MAPK/NFkappaB. Int Immunopharmacol 2018; 55: 69-76.